의학석사 학위논문

Modeling of measurement error range in lung nodule volumetry

Prospective study with same day repeat computed tomography for metastatic lung nodules

폐결절 용적측정의 측정 오차 범위 모델링

전이성 폐결절의 당일 반복 전산화 단층 촬영을 통한 전향적 연구

2014 년 8 월

서울대학교 대학원

의학과 영상의학전공

황 의 진

A thesis of the Degree of Master of Science in Medicine

폐결절 용적측정의 측정 오차 범위 모델링

전이성 폐결절의 당일 반복 전산화 단층 촬영을 통한 전향적 연구

Modeling of measurement error range in lung nodule volumetry

Prospective study with same day repeat computed tomography for metastatic lung nodules

July 2014

The Department of Radiology,
Seoul National University
College of Medicine
Eui Jin Hwang

Modeling of measurement error range in lung nodule volumetry

Prospective study with same day repeat computed tomography for metastatic lung nodules

폐결절 용적측정의 측정 오차 범위 모델링

전이성 폐결절의 당일 반복 전산화 단층 촬영을 통한 전향적 연구

지도 교수 구 진 모

이 논문을 의학석사 학위논문으로 제출함

2014년 04월

서울대학교 대학원

의학과 영상의학 전공

황 의 진

황의진의 의학석사 학위논문을 인준함

2014년 07월

위 원 장 _____ (인)

부위원장 _____ (인)

위 원 _____ (인)

Abstract

Introduction: Semi-automated lung nodule volumetry is a promising tool for early detection of volume change, which might led to early diagnosis of malignancy and treatment failure. Measurement variability in volumetry is known to be affected by various factors. The purpose of our study was to model the range of variability in lung nodule volumetry, in patient with metastatic lung nodules by same day repeat computed tomography (CT) scans

Methods: The present prospective study included 50 patients with known pulmonary metastatic nodules between November 2013 and April 2014, with written informed consents. Two consecutive noncontrast chest CT scans were performed within 10 minutes of time interval. Non-calcified nodules with diameter between 4mm and 15mm were segmented using in-house software for each CT scans. After calculation of mean segmented nodule volume (V_m), surface voxel proportion (*SVP*) was defined as the proportion of surface voxels in total segmented voxels, while attachment proportion (AP_N) was defined as the proportion of voxels with greater attenuation than *N* in total voxels just outside of surface of nodule. Absolute percentage error (*APE*) and relative percentage error (*RPE*) were calculated from segmented nodule volume on each CT scans. Univariate and multivariate quantile regression analyses were performed for estimation of 95% upper limit of *APE*.

Results: The 95% limits of variability of *RPE* was from -20.81% to 20.62%. In univariate quantile analyses, V_m, Sphericity, *SVP,* AP_{-700} and AP_{-600} were significant variables for estimation of *APE*. In multivariate analysis, *SVP* and

AP_{-700} were proven to be independently significant variable and final model for 95% limit of *APE* was as follows: $APE = 46.01 \cdot SVP + 36.32 \cdot AP_{-700} - 12.94$.

Conclusions: In conclusion, *SVP* and *AP* were independent factors for variability in lung nodule volumetry. With those two parameters, 95% limit of absolute percentage error in lung nodule volumetry could be estimated with linear model.

Keywords: Computed tomography, Lung nodule, Measurement error, Volumetry, Modelling
Student Number: 2012-23629

CONTENTS

LIST OF TABLES AND FIGURES

LIST OF ABBREVIATION

AP = Attachment proportion

AP_N = Attachment proportion with threshold Hounsfield unit of N

APE = Absolute percentage error

CT = Computed tomography

HU = Hounsfield unit

RECIST = Response evaluation criteria in solid tumors

RPE = Relative percentage error

SVP = Surface voxel proportion

V_m = Mean segmented nodule volume

INTRODUCTION

Pulmonary nodules are the most common manifestation of primary and secondary pulmonary malignancies (1). Size measurements and assessment of size change are used for prediction of likelihood of malignancy of nodule (2) and monitoring of response of tumor to treatment (3). Accurate measurement of pulmonary nodule is required to identify interval change of nodule size in short time interval. However, conventional one-dimensional measurement of pulmonary nodules is prone to measurement error, especially in small nodules (4, 5). The Response Evaluation Criteria in Solid Tumors (RECIST) version 1.1, the current standard method for treatment response monitoring, provides 20% of relative change and 5 mm of absolute change for definition of progressive disease (6).

Volumetric measurement of pulmonary nodules, might provide more accurate and consistent measurement, and therefore lead to better identification of interval change of nodule volume and early diagnosis of malignant nodule or treatment failure (7-9). A number of previous studies were performed to assess the measurement variability of lung nodule volumetry and reported relative measurement variability up to 20% to 25% (10-13). In addition, a variety of studies have reported there are various factors that affect measurement variability, including nodule characteristics, scanning and reconstruction parameters and patient-related factors (14-17).

In Dutch-Belgian lung cancer screening trial, semi-automated lung

nodule volumetry was used for measurement of lung nodule and 25% volume change was adopted as threshold for nodule growth (18). However, the threshold was set up en bloc, without considering various nodule characteristics that affect the range of variability. If we can diversify the threshold according to nodule characteristics, earlier identification of significant volume change can be made for nodules with low estimated threshold, furthermore, tailored diagnostic approach can be given with different estimated variability. However, there has been no study that tries to estimate the range of variability with associated nodule characteristics.

Because the uncertainty in lung nodule segmentation mainly arises in surface of the nodule, surface voxels, which located at the interface of nodule and lung parenchyma, may play key role in segmentation variability (19). Surface voxels are affected by partial volume averaging effect with lung parenchyma, so that may segmented either as nodule or as parenchyma. Therefore, larger proportion of surface voxel to total voxels of nodule may result in greater variability. In addition, attachment between nodule and other anatomic structures such as pulmonary vessels and chest wall also cause uncertainty in segmentation. Greater portion of attachment with other structure may cause larger variability.

Therefore, the purpose of our study was to model the variability of lung nodule volumetry in patient with metastatic lung nodules by same day repeat CT scans.

MATERIALS AND METHODS

Patient selection

The present study was approved by our institutional review board and written informed consents were obtained from all the patients after explanation of additional radiation dose.

Between November 2013 and April 2014, a total of 50 patients (26 male and 24 female; mean age 62.6 years, ranging from 32 years to 82 years) were prospectively included in the present study with following inclusion criteria: (a) patients with known metastatic pulmonary nodule with diameter of 4 mm or greater; (b) patients who referred for follow-up noncontrast chest CT; (c) patients without active pulmonary symptoms such as cough, sputum, or dyspnea. Underlying primary tumors were described in table 1.

Table 1. Primary tumors of metastatic pulmonary nodules

Primary tumor	Patient number
Renal cell carcinoma	13
Thyroid cancer	8
Lung cancer	6
Colorectal cancer	4
Hepatocellular carcinoma	3
Adenoid cystic carcinoma	3
Benign metastasizing leiomyoma	3
Malignant melanoma	1
Bladder cancer	1
Chondrosarcoma	1
Thymic carcinoma	1
Endometrial cancer	1
Breast cancer	1
Malignant fibrous histiocytoma	1
Unknown	3

Image acquisition

We performed two sequential chest CT examinations without contrast enhancement for each patient. All scans were performed with a single 64-channel multi-detector CT (Brilliance 64, Philips, Eindhoven, Netherlands) with patients in supine position with full inspiration. Scanning parameters were as follows: (a) tube voltage and reference tube current of 120 kVp and 200 mAs; (b) detector collimation of 0.625 mm x 64; (c) spiral pitch of 0.515. First scans covered from lower neck to costophrenic angle for clinical indication, while second scans covered only areas with metastatic nodules to minimize radiation dose. The time interval between two CT scans were less than 10 minutes, and patients left the table between two scans. Axial images were reconstructed with slice thickness/increment of 1mm/1mm, with non-enhanced medium sharp reconstruction filter (YC). Fields-of-views (FOVs) were set to cover whole thoracic cage (average FOV 308.5mm, ranging from 277 mm to 379 mm) and matrix numbers were 512 by 512.

Average ± standard deviation dose-length product for first and second CT scans were 332.7 ± 92.6 mGy·cm and 265.5 ± 96.5 mGy·cm, respectively. Considering conversion factor 0.0145 for 120 kVp chest CT in adults, average ± standard deviation for first and second scans were 4.82 ± 1.34 mSv and 3.85 ± 1.40 mSv, respectively.

Nodule selection

For selection of pulmonary nodules for volumetry, one radiologist (E.J.H., 3 years of experience in thoracic radiology) reviewed obtained images and annotated candidate nodules for volumetry. Nodules with diameter between 4 mm and 15 mm were included in the study. Nodules with internal calcification or cavitation were excluded because internal high variation of attenuation may cause error in volumetry. Nodules that are significantly affected by motion artifact were also excluded. Finally a total of 1259 nodules (average 25.2 nodules per patient, ranging from 1 to 148 nodules per patient) were identified for volumetry.

Segmentation and volume measurement of nodules

Semi-automated lung nodule segmentations and volume measurements were performed with our in-house software (Figure 1). After identification of target nodule, rectangular ROI was drawn at representative slice. The iso-center point of ROI was given as the seed point for segmentation. With threshold of -400 Hounsfield units (HU), nodules were segmented from lung parenchyma with lesion growing method. Afterwards, surrounding vascular structures and chest wall were removed from segmented nodule with rolling-ball algorithm (20). Figure 1 show an example of segmentation. One radiologist visually assessed the result of segmentation. When estimated mismatch between the nodule and segmented volume was greater than 20% (poor segmentation) or segmentation was totally failed, we excluded the nodule from the analyses

(21). (Figure 2)

Segmentations were performed for each target nodule, in two CT scans. Following data are collected based on the results of each segmentation: (1) Volume of segmented nodule (mm^3); (2) Surface area of segmented nodule (mm^2); (3) Number of total segmented voxels; (4) Number of surface voxels; (5) Voxel size (mm^3); and (6) Attenuation histogram of outer voxels that attached to the surface of segmented nodule. After acquisition of aforementioned data, we calculated following additional data: (1) Surface voxel proportion (*SVP*); (2) Attachment proportion (*AP*); (3) Sphericity; (4) Absolute percentage error (*APE*, %) and (5) Relative percentage error (*RPE*, %). Equation for each calculated data are as follows:

$$SVP = \frac{Number\ of\ surface\ voxels}{Number\ of\ total\ segmented\ voxels}$$

$$AP_N = \frac{Number\ of\ outer\ voxels\ with\ HU\ greater\ than\ N}{Number\ of\ total\ outer\ voxels}$$

$$Sphericity = \frac{\pi^{\frac{1}{3}} \cdot (6Volume)^{\frac{2}{3}}}{Surface\ area} \quad (22)$$

$$Absolute\ percentage\ error\ (\%) = \frac{|V_1 - V_2|}{V_m} \cdot 100$$

$$Relative\ percentage\ error\ (\%) = \frac{V_1 - V_2}{V_m} \cdot 100$$

where V_1, V_2 and V_m means segmented nodule volume at 1st, 2nd scan and its average.

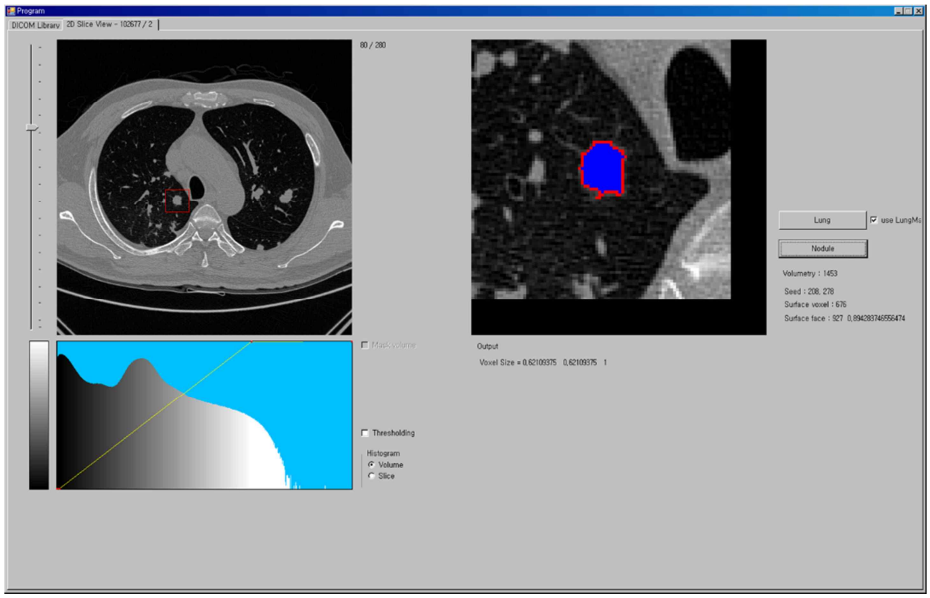

Figure 1. An example of lung nodule segmentation

Semi-automated lung nodule segmentation was done for a nodule in right upper lobe, in a 48-year-old female patient with renal cell carcinoma with lung metastasis. Red-colored voxels indicate surface voxels of segmented nodule.

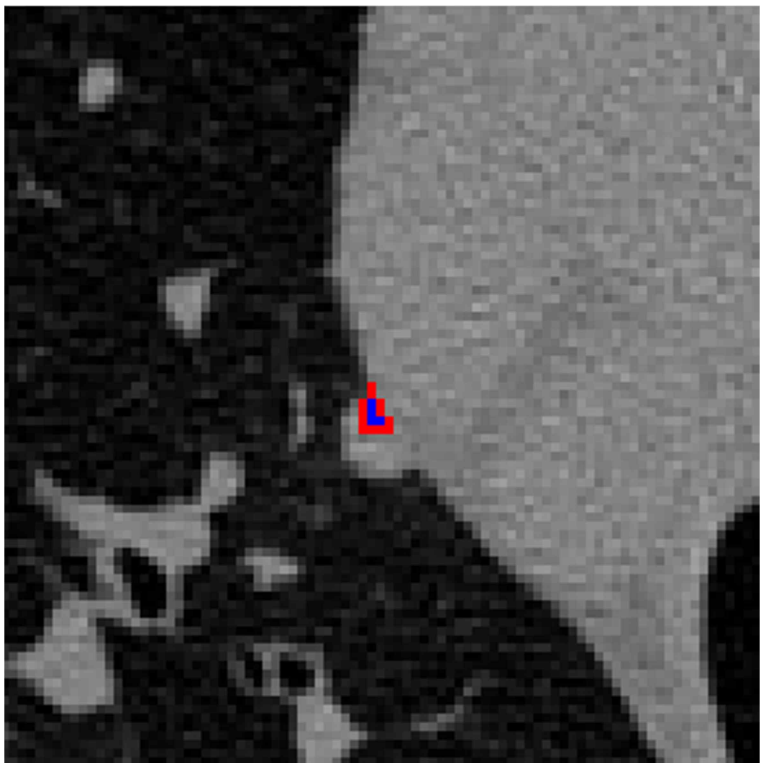

Figure 2. An example of poor segmentation

Semi-automated segmentation was done for a nodule attached to mediastinal pleura in a 71-year-old male patient with metastatic renal cell carcinoma. Segmented area covered only small part of the nodule. When gross mismatch between segmentation result and nodule is greater than 20%, nodules were excluded from the analyses.

Statistical analyses

All the statistical analyses were performed with R software (version 3.1.0; R project) and IBM SPSS statistics (version 20.0, IBM, Armonk, NY). To assess degrees and patterns of *RPE* with various factors, Bland–Altman plots were derived. After gross assessment of patterns of *APE* with scattered plots, univariate and multivariate quantile regression analyses were performed for development of the model which estimate 95% quantile of *APE* (23, 24). Results with *P*-values <0.05 were considered to be statistically significant.

RESULTS

Table 2 shows descriptive statistics for volumetric data. The 95% limit of agreement for *RPE* was -20.81% to 20.62%.

Table 2. Descriptive statistics of volumetric data

Variable	Average ± SD (Range)
V_m (mm^3)	174.22 ± 271.91 (10.09 – 3870.06)
Sphericity	0.739 ± 0.072 (0.514 – 0.906)
Voxel size (mm^3)	0.354 ± 0.057 (0.284 – 0.548)
SVP	0.650 ± 0.151 (0.240 – 0.934)
AP_{-700}	0.102 ± 0.082 (0 – 0.566)
AP_{-600}	0.053 ± 0.065 (0 – 0.491)
AP_{-500}	0.020 ± 0.037 (0 – 0.264)
APE (%)	7.18 ± 7.75 (0 – 59.22)

*Abbreviation: V_m, mean volume of segmented nodule; *SVP*, surface voxel proportion; *AP*, attachment proportion; *APE*, absolute percentage error

Bland-Altman plots for error pattern analyses

Figure 3 show Bland - Altman plots for *RPE* according to volumetric variables. *RPE*s show trend to increase with increasing *SVP* and decreasing sphericity and V_m. For *AP*, we tested various thresholds, i.e., -700, -600, -500 HU. However, we observed no remarkable difference among various thresholds.

(A)

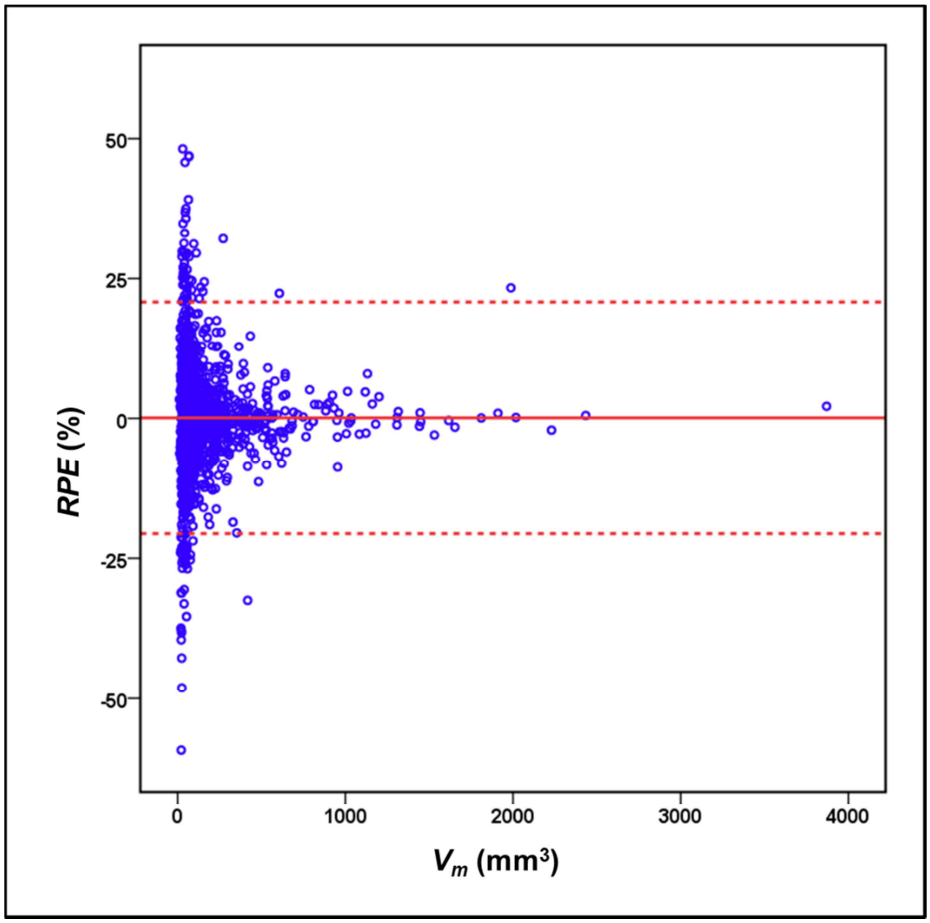

(B)

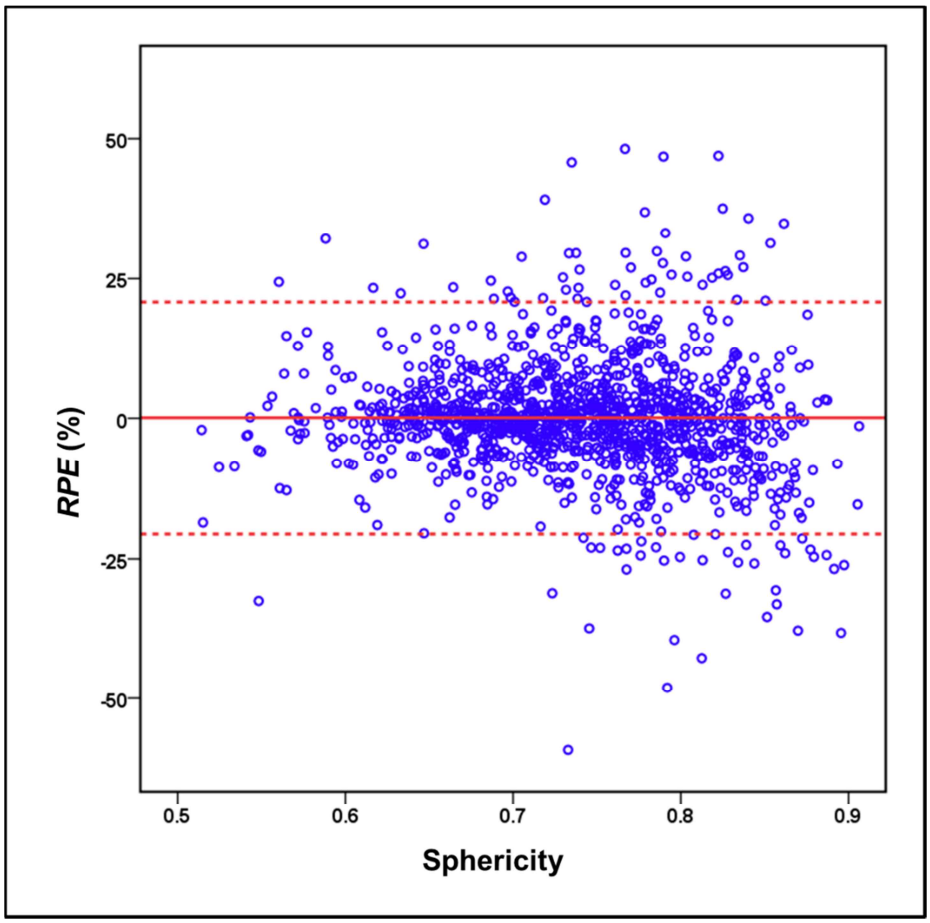

(C)

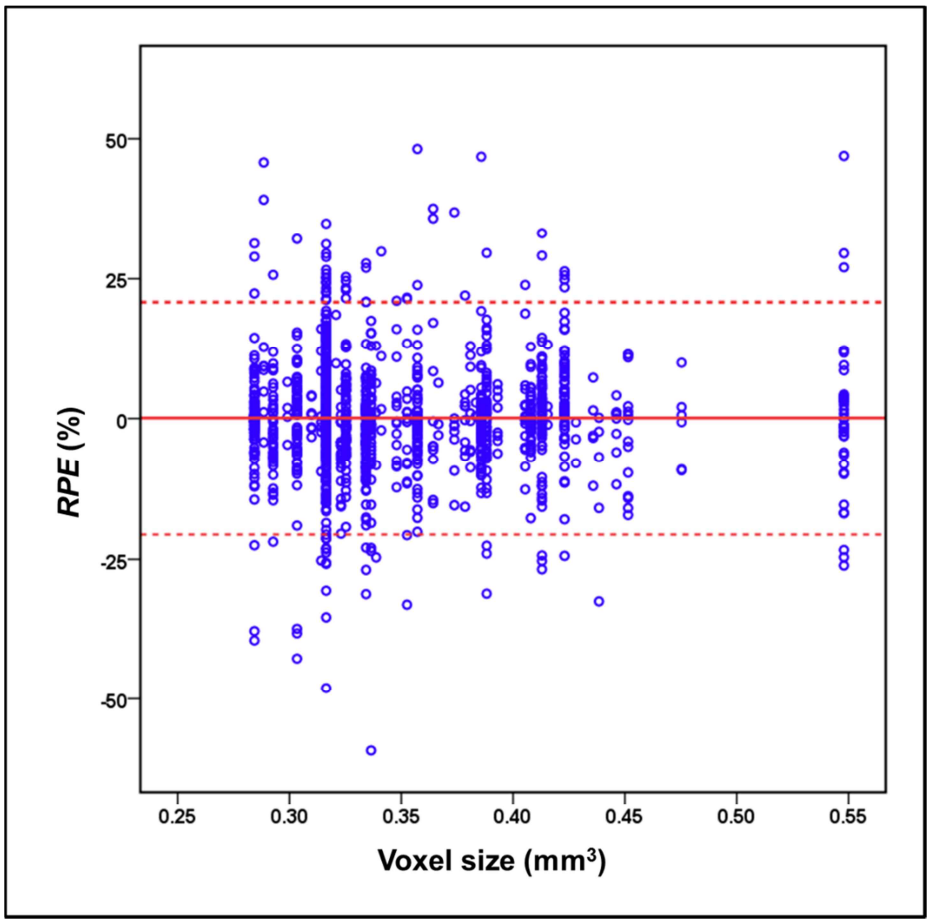

(D)

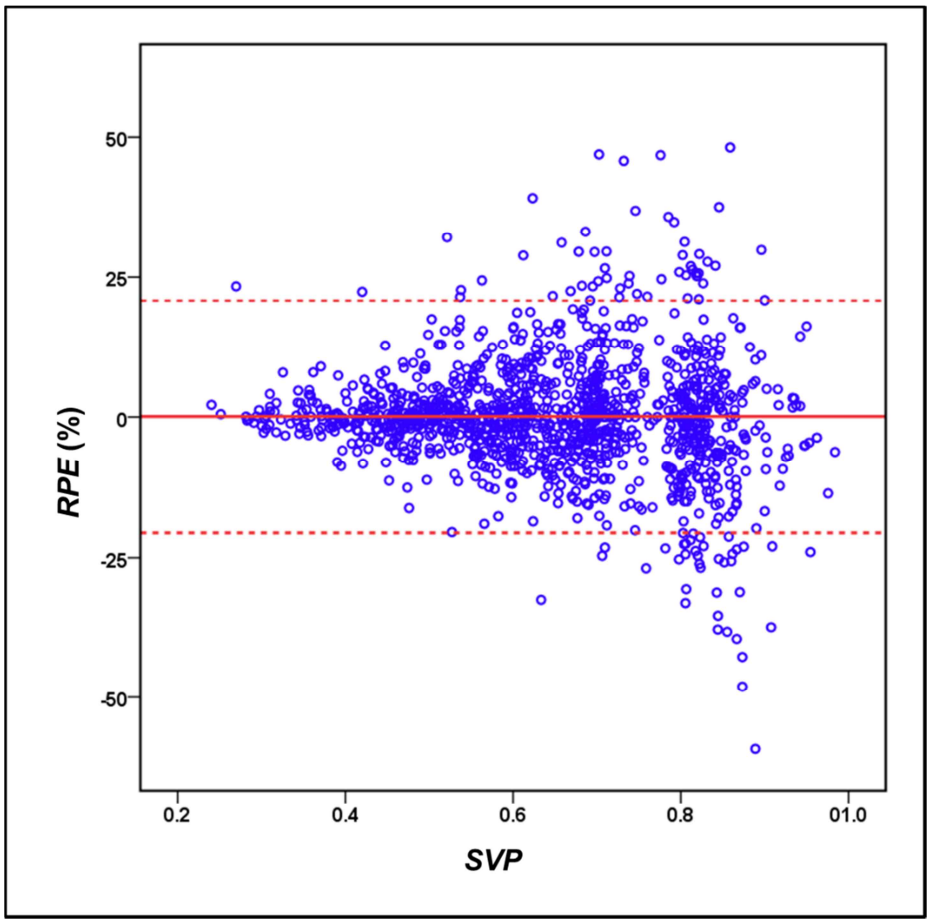

(E)

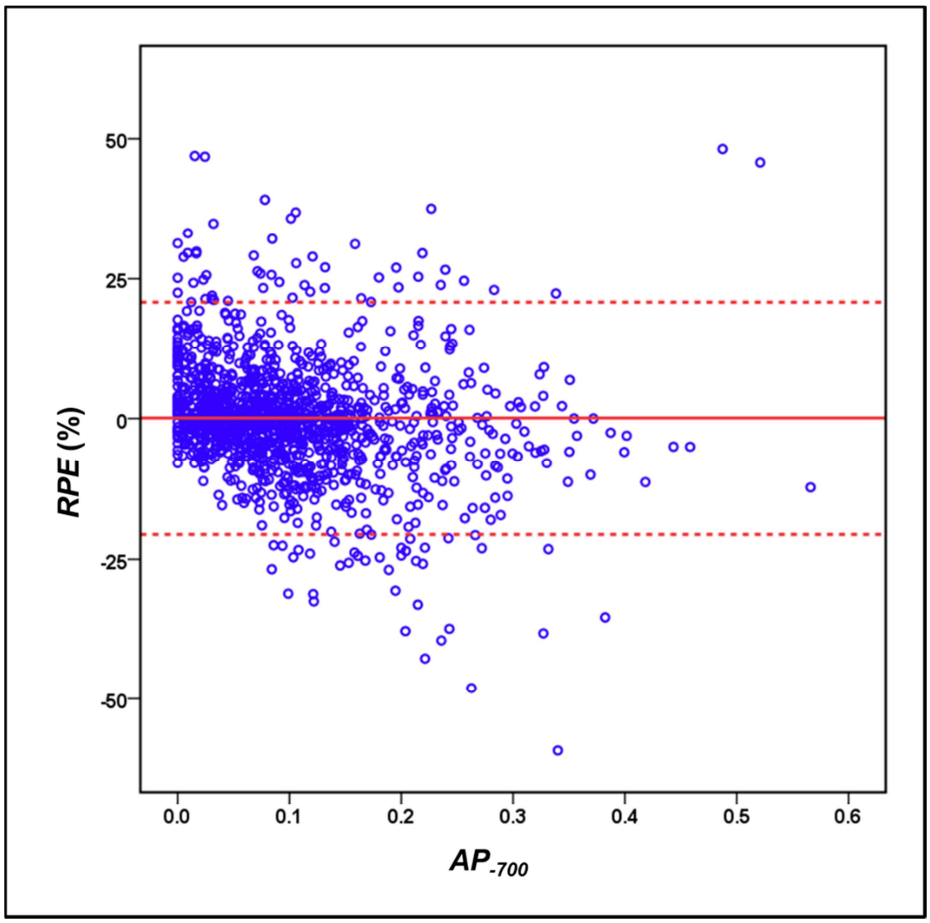

(F)

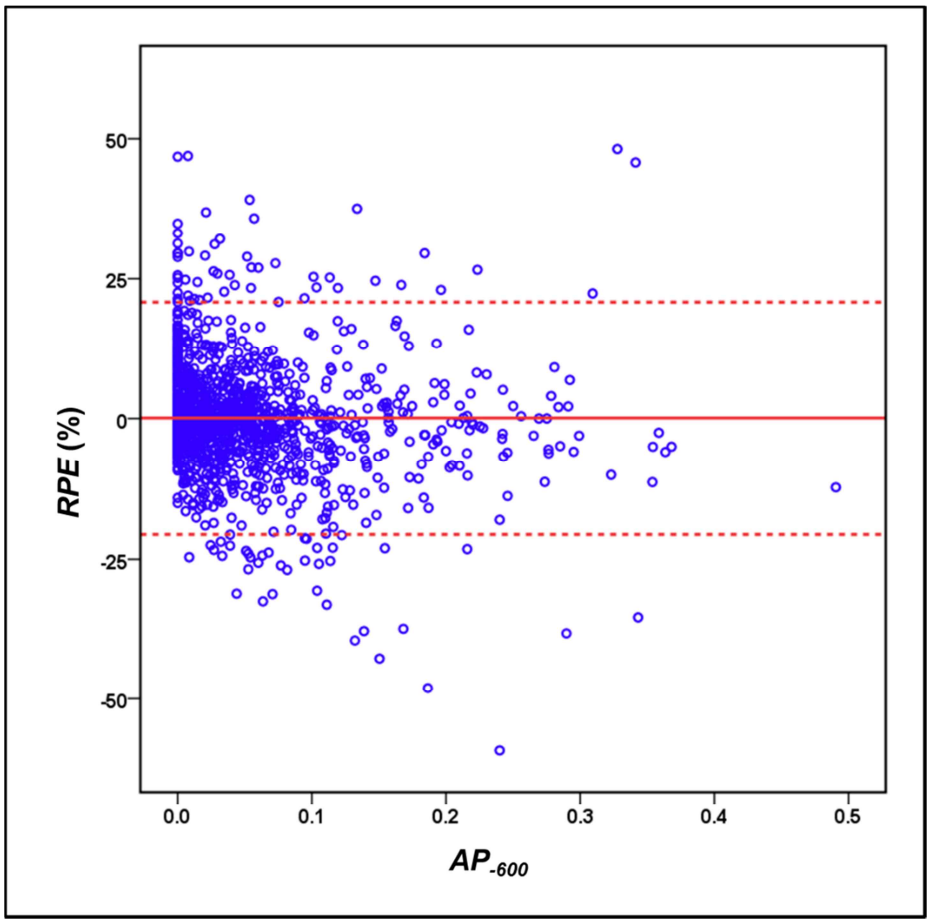

(G)

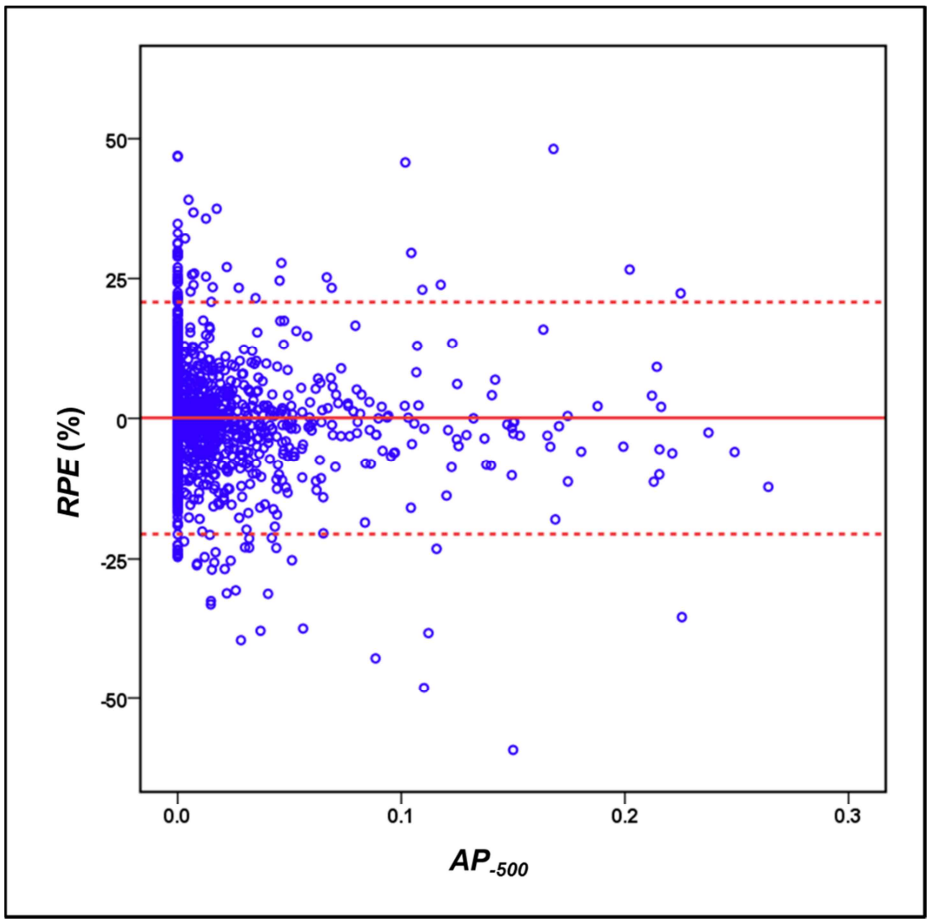

Figure 3. Bland-Altman plots for *RPE* according to various volumetric parameters.

The range of *RPE* tended to increase with (A) decreasing V_m, (B) increasing sphericity. (C) No definite tendency was observed for voxel size while (D) the range of *RPE* goes greater with increasing *SVP*. (E-G) For *AP,* the range of *RPE* tended to increase with increasing AP_{-700}, AP_{-600} and AP_{-500}. No remarkable difference was observed among three different thresholds for *AP*.

Univariate quantile regression analyses

To estimate upper 95% limit of *APE*, we inserted V_m, *SVP*, sphericity, voxel size and AP_{-700}, AP_{-600}, AP_{-500} as independent variables for univariate quantile analyses. For V_m, logarithmic transformation was performed for linear fitting. Table 3 shows results of analyses. As a result, V_m, *SVP*, Sphericity, AP_{-700} and AP_{-600} were appeared to be significant variables. However, voxel size and AP_{-500} were not significant variable for estimation of *APE*. Figure 4 show scattered diagrams and estimation line for 95% quantile of *APE*.

Table 3. Univariate quantile regression analyses for 95% quantile of *APE*

Variable	Coefficient	*P*-value	Intercept	*P*-value
Log V_m (mm^3)	-6.2	<0.001	49.41	<0.001
Sphericity	54.41	0.027	-17.87	<0.001
Voxel size (mm^3)	10.43	0.562	19.95	<0.001
SVP	47.95	<0.001	-10.29	<0.001
AP_{-700}	56.57	<0.001	16.31	<0.001
AP_{-600}	77.15	<0.001	19.45	<0.001
AP_{-500}	129.82	0.055	21.61	<0.001

*Abbrevation: *APE*, absolute percentage error; V_m, mean volume of segmented nodule; *SVP*, surface voxel proportion; *AP*, attachment proportion

(A)

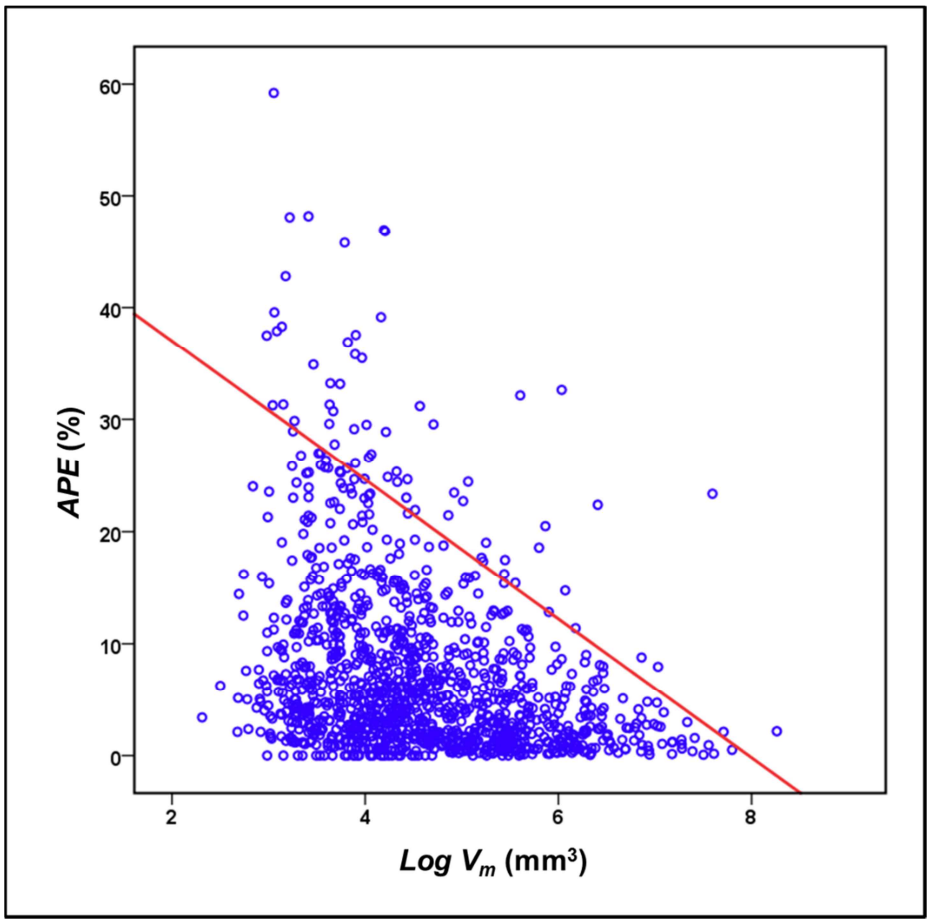

(B)

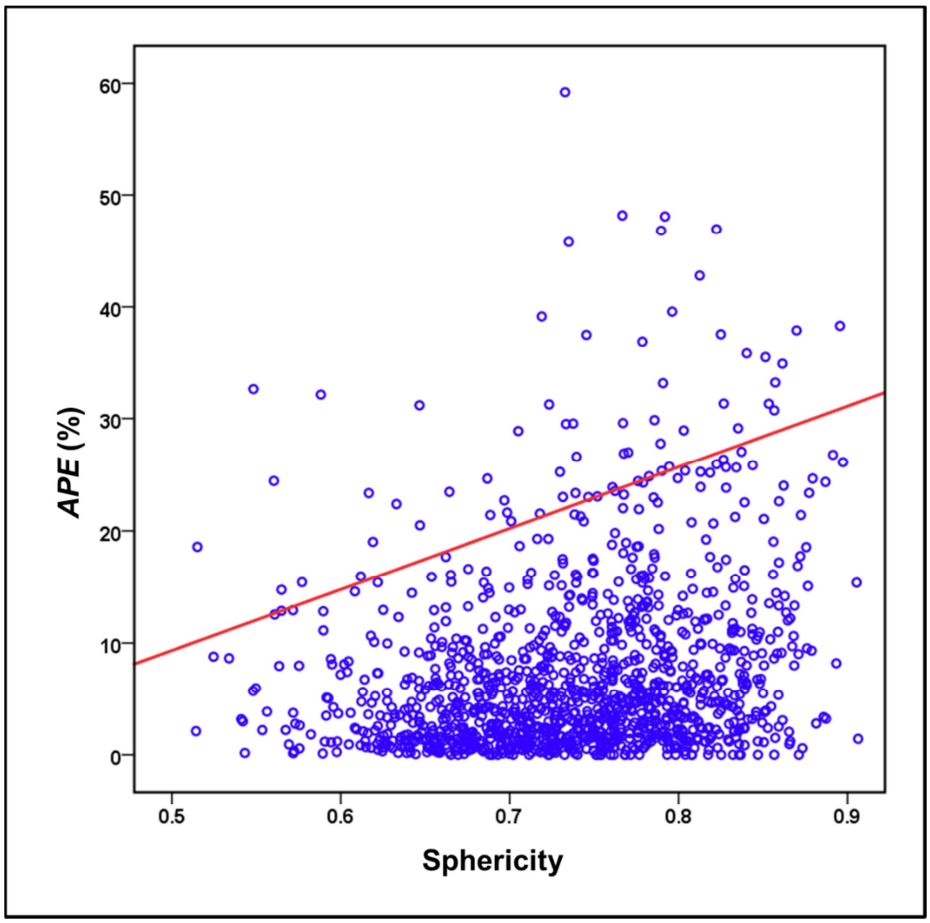

(C)

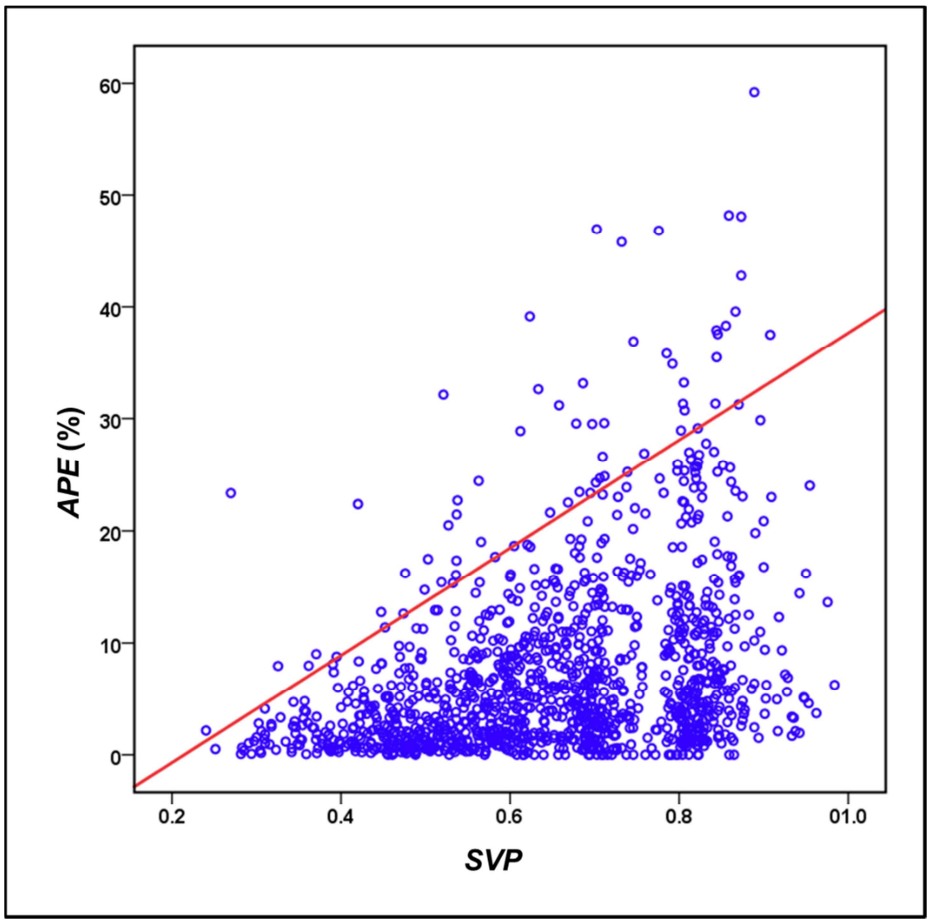

(D)

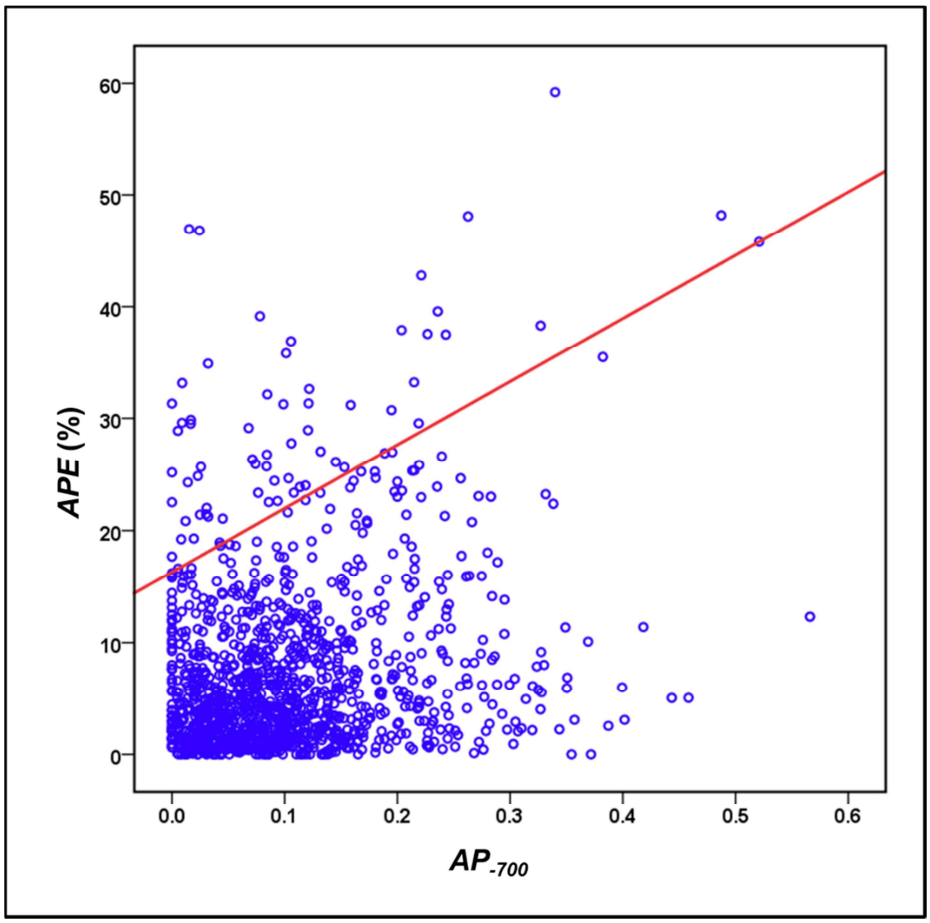

(E)

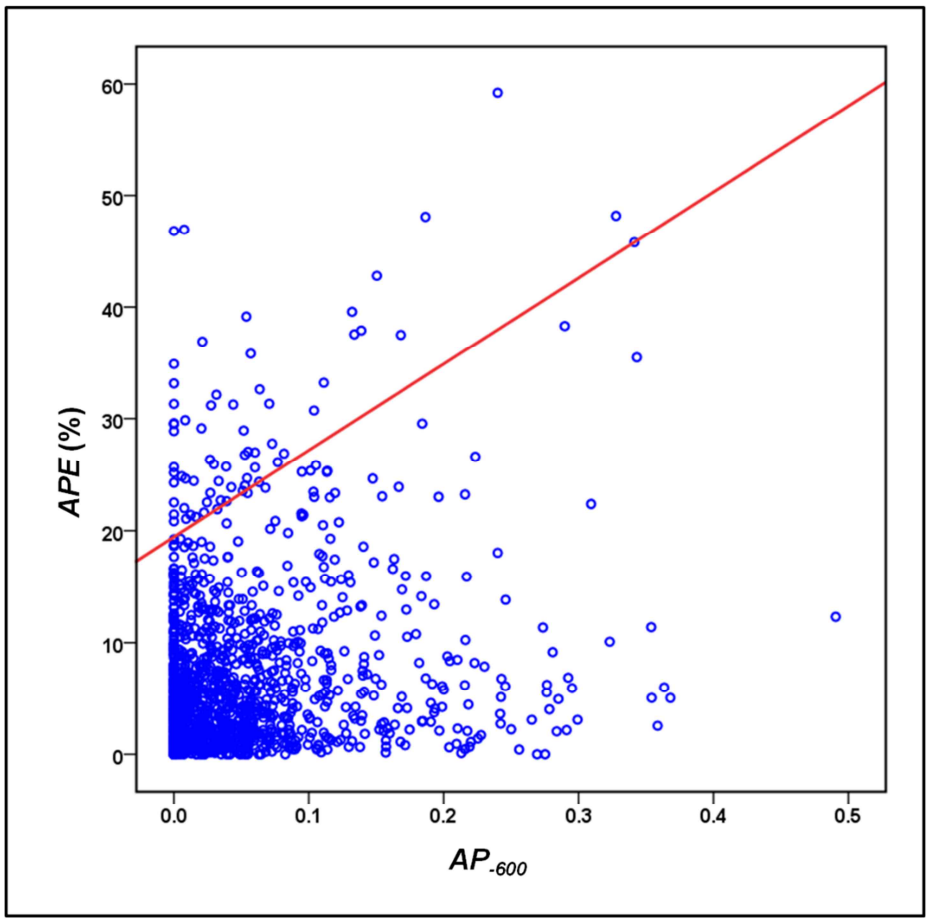

Figure 4. Scattered plots for volumetric parameters and *APE* with estimation for 95% quantile of *APE*.

(A) The 95% quantile of *APE* increased with decreasing Log V_m and (B) increasing sphericity. We also observed increasing 95% quantile of *APE* with increasing (C) *SVP*, (D) AP_{-700}, and (E) AP_{-600}. Red-colored line indicate 95% quantile of *APE*.

Multivariate quantile regression analysis

We performed multivariate analysis using variables appeared to be significant in univariate analyses. V_m and AP_{-600} were excluded from the multivariate analyses because of multicolinearity. Finally, *SVP*, sphericity and AP_{-700} were input variables. As a result, *SVP* (P <0.001), and AP_{-700} (P <0.001) were proven to be independent significant variables for estimation of upper 95% quantile of *APE*. Final equation for estimation of 95% quantile of *APE* is as follows:

$$APE = 46.01 \cdot SVP + 36.32 \cdot AP\_{-700} - 12.94$$

Based on the model, mean ± standard deviation of estimated 95% quantile of *APE* was 20.67 ± 7.89%, ranging from 1.03% to 49.85%. Among 1260 nodules, 1194 nodules (94.84%) showed observed *APE* smaller than estimated 95% quantile of *APE*. Meanwhile, 851 nodules (67.5%) showed estimated 95% quantile of *APE* smaller than 25%. Figure 5 shows histogram for estimated 95% quantile of *APE*.

Figure 6 and 7 show CT images of representative nodules.

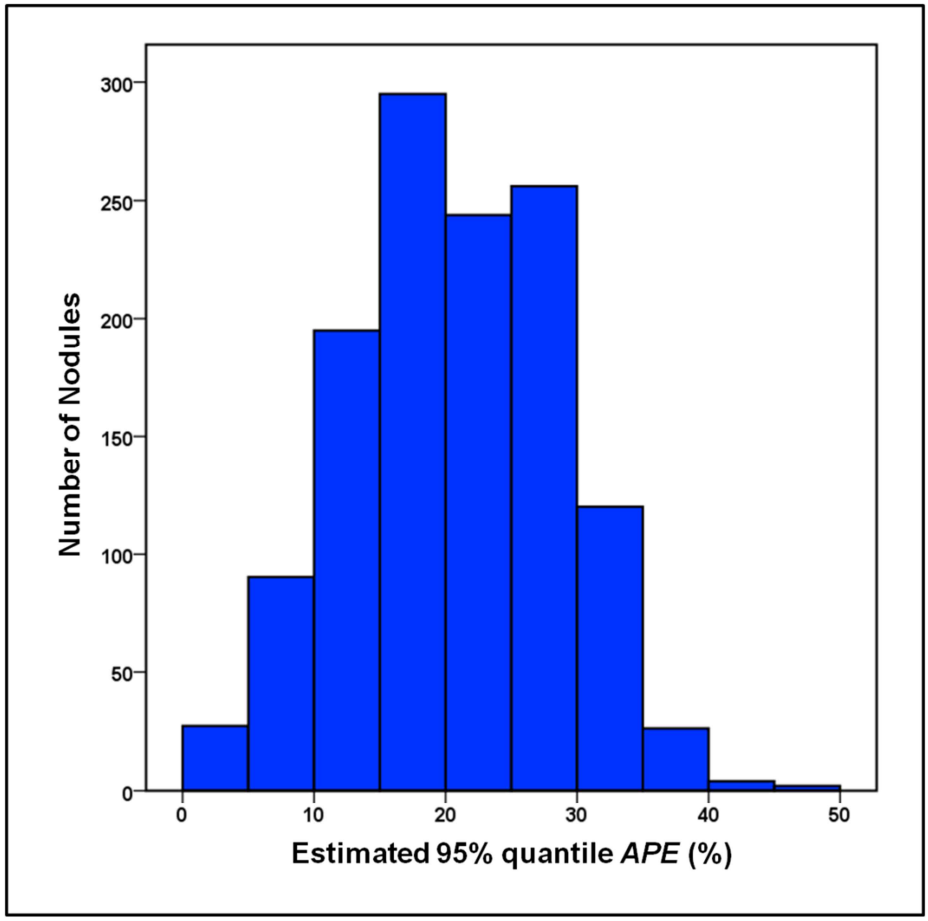

Figure 5. Histogram of estimated 95% quantile of *APE*

Average estimated 95% quantile of *APE* was 20.67%. A total of 52.4%, 67.5% and 88.2% of nodules were estimated to have 95% quantile *APE* smaller than 20%, 25% and 30%, repectively.

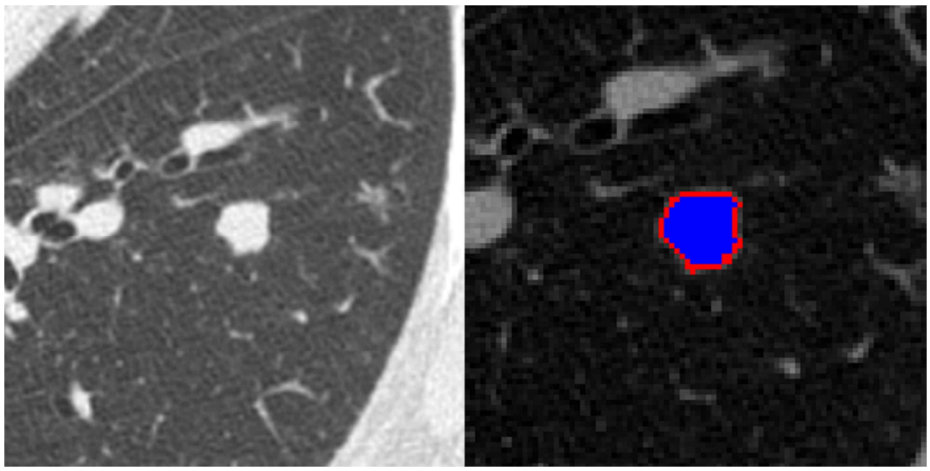

Figure 6. An example of nodule volumetry with *APE* of 1.56%

Volumetry was performed for a nodule in left lower lobe in a 53-year-old male patient with metastatic renal cell carcinoma. V_m was 416 mm^3, while *SVP* and AP_{-700} were 0.450 and 0.059, respectively. Estimated 95% quantile of *APE* was 9.91%

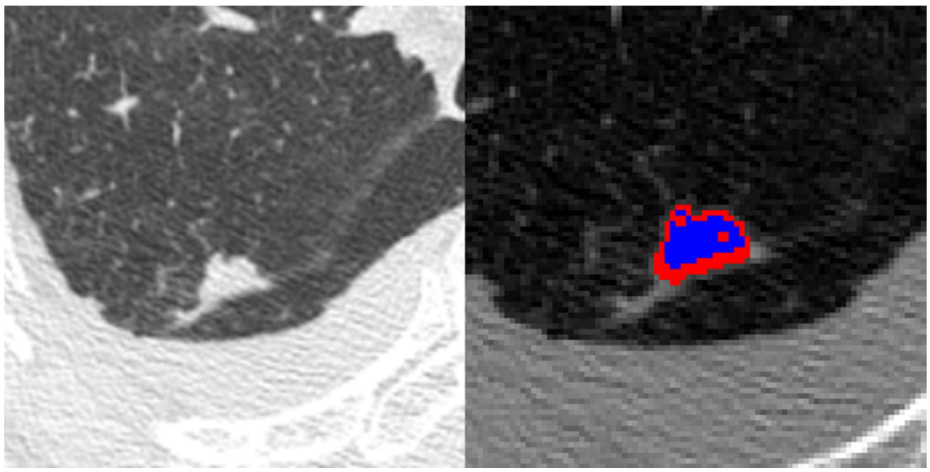

Figure 7. An example of nodule volumetry with *APE* of 32.6%

Volumetry was performed for a nodule attached to right major fissure in a 75-year-old male patient with metastatic renal cell carcinoma. V_m was 417 mm^3, while *SVP* and AP_{-700} were 0.633 and 0.122, respectively. Estimated 95% quantile of *APE* was 20.62%

DISCUSSION

Semi-automated volumetric measurement of pulmonary nodules has been emerged as promising method for evaluation of small pulmonary nodules because of potential usefulness in detection of small nodule volume change, which lead to early identification of malignant lung nodule or response of nodules to specific treatment (19, 25). Estimation of variability in volumetric measurement is crucial in differentiation of true nodule volume change from measurement error. In the present study, we found *SVP* and *AP* as the independent estimating factor for variability in lung nodule volume measurement.

Considering the range of *RPE*, our study showed 95% limits of agreements of -20.81% to 20.62%, which was comparable or even smaller than results of other previous studies (10-13). Exclusion of small nodules with diameters <4mm might be one of causes of rather low variability.

In the present study, we were interested in the upper limit of *APE*, rather than its average value. Therefore, we utilized quantile regression analyses, rather than conventional linear regression analyses with least squares method. Quantile regression analyses give more complete understanding of the pattern of relation between variables in each percentile of dependent variable. Moreover, it does not require

normality or homoscedasticity and it is much less influenced by outliers. (23, 24)

Variability in lung nodule segmentation arises from the surface of the nodule. Surface voxel is composed with partial volumes of both nodule and lung parenchyma, therefore, whether surface voxel is included in the segmentation or not is the key for variability in lung nodule volumetry. Therefore we hypothesized the proportion of surface voxel in segmented nodule, in other ward, *SVP*, should be a powerful estimating factor for variability in volumetry.

Nodule size, voxel size and nodule shape are well-known variables that cause variability in volumetry (8, 14, 16, 17, 26). In the present study, nodule size, represented by V_m and nodule shape, represented by sphericity appeared to be significant factor for *APE*. However, voxel size did not appear to be significant variable. This is probably due to rather small range of voxel size distribution and selection of multiple nodules in single patient. Those three variables, nodule size, nodule shape and voxel size can be integrated with *SVP*. Increasing volume of nodule with same voxel size may cause decrease in *SVP*, while increasing size of voxel with same nodule volume may cause increase in *SVP* (Figure 8). In the same manner, elongated, non-spherical nodule may have high *SVP* rather than round, spherical nodule when they have same volume, therefore might be related with

high variability. In univariate analysis in the present study, *SVP* was proven to be a significant estimating factor for *APE*. Also in multivariate analyses, *SVP* was independent estimating factor for *APE*, while sphericity was eliminated.

Interestingly, we found tendency of increasing *APE* with increasing sphericity on univariate quantile analysis. Sphericity is a measure of how spherical an object is (22). Therefore, increasing sphericity of nodule should have been associated with decreased *APE*. The paradoxical result of the present study might be due to confounding effect of nodule volume. Small nodules tend to be more spherical in shape, while larger nodules usually have attachment with other structures and show more irregular shape. In the present study, sphericity showed strong negative correlation with Log V_m (r=-0.738, P<0.001, Pearson's correlation test).

Another key factor for variability in lung nodule segmentation is attachment between nodule and other structures. Pulmonary vessels, mediastinum and chest wall are typical anatomic structures that often show attachment with pulmonary nodules. Those structures have similar attenuation with nodules, therefore, segmentations of those structures are more prone to error than segmentations of lung parenchyma, which have much lower attenuation than nodules (27, 28). We assumed that among voxels located at just outside of surface of

nodule, voxels with higher attenuation than lung parenchyma may indicate attachment with other structures. Therefore, we hypothesized *AP*, which indicates the proportion of voxel with higher attenuation than lung parenchyma among outside voxels adjacent to surface of nodule, should be another factor for variability in volumetry. We applied three different thresholds for definition of attachment. In Bland-Altman plots, there was no significant difference in error patterns among different thresholds, while nodules with zero *AP* are increased. Therefore, we adopted threshold of -700 HU for quantile regression analyses. With increasing *AP*, we observed a tendency of increasing range of APE. In univariate and multivariate quantile regression analyses, AP_{-700} was an independent estimating factor for 95% quantile of *APE*.

With multivariate quantile regression analyses, we developed a model for estimation of 95% limit of *APE*. Two variables, i.e. *SVP* and AP_{-700}, and constant term were included in the equation. Therefore, with simple substitution of *SVP* and AP_{-700}, 95% limit of *APE* can be achieved. Furthermore, those two parameters are easily acquired with our volumetric software. Assuming the situation of pulmonary nodule follow up with volumetry, 95% limit of *APE* as well as volume of target nodule can be acquired with volumetric software. If the volume change of the target nodule exceeds the 95% limit of *APE*, one might conclude

that the volume of nodule has been truly changed.

Determination of timing for follow-up CT to identify interval growth of nodule is critical in clinical settings of pulmonary nodule management. Critical time for follow-up CT to identify meaningful nodule growth can be determined by defining volume change threshold for reliable volume change and doubling time threshold between growing and stable nodule (29). Therefore, tailored nodule management can be given by adjusting follow-up CT interval if we can estimate thresholds for meaningful volume change in each nodule. The estimated 95% quantile of *APE* in our model can be a potential candidate for the tailored threshold.

In the present study, 67.5% of nodules showed estimated 95% limit of *APE* smaller than 25%. Therefore, by applying estimated value as threshold for true nodule volume change, early detection of volume change can be made in those nodules compared with giving single threshold of 25%. On the other hand, for the other 32.5% of nodules with estimated 95% quantile of *APE* greater than 25%, longer follow-up interval can be applied to detect true nodule growth. Therefore, unnecessary radiation exposure due to early follow up CT scan can be prevented.

The present study has several limitations. First, several nodule-related and patient-related factors were ignored in the present study. For

example, attenuation of nodule was not considered in the present study. Decreased nodule attenuation leads to decreased contrast between nodule and lung parenchyma, therefore, may cause increased error in volumetry. Nodules with ground-glass opacity have been reported to have larger error in volumetry (15). In the present study, only solid, non-calcified nodules were included for the analyses, the effect of nodule attenuation may hold only small effect. One of the most patient-related factors in variability is degree of inspiration (30, 31). Because our volumetric software use threshold value of -400 HU, we expect degree of inspiration cause only small variability (10). However, further study is required for evaluation of the degree of variability caused by different degree of inspiration. Second, variability modeling was performed in basis of same CT scanning and reconstructing parameters. A variety of scanning and reconstructing parameters are known to cause variability in volumetry (14, 15, 27). Some of those parameters can be integrated with *SVP*, such as slice thickness and matrix size, however, other prameters such as image noise, which affected by radiation dose or reconstruction algorithm, cannot be explained with *SVP*. Therefore, further studies including variable scanning and reconstruction parameters would be required for further evaluation. Third, quantification of attachment of nodule with other structures was performed with only attenuation-based ratio. The method have

limitation because it does not consider the clustering of attached voxels. For example, attachment with multiple small-sized vessels and single large-sized vessel may similar *AP* in the present study, however, the effect on volumetric error may quite different. Therefore, further study with different method for quantification of attachment that can reflect the clustering pattern of attachment may be required. Finally, only metastatic nodules were included in the present study. Primary lung cancers appearing as pulmonary nodules, which usually show irregular shape and margin, may have larger intrinsic variability (32). Further studies would be required to prove whether the result of present study is reproducible in primary lung cancer nodules.

In conclusion, *SVP*, which indicate the proportion of uncertainty in volume of pulmonary nodule, and *AP*, which indicate the proportion of attachment between nodules and surrounding structures, were independent factor for variability in lung nodule volumetry. With those two parameters, 95% limit of absolute percentage error in lung nodule volumetry could be estimated with linear model.

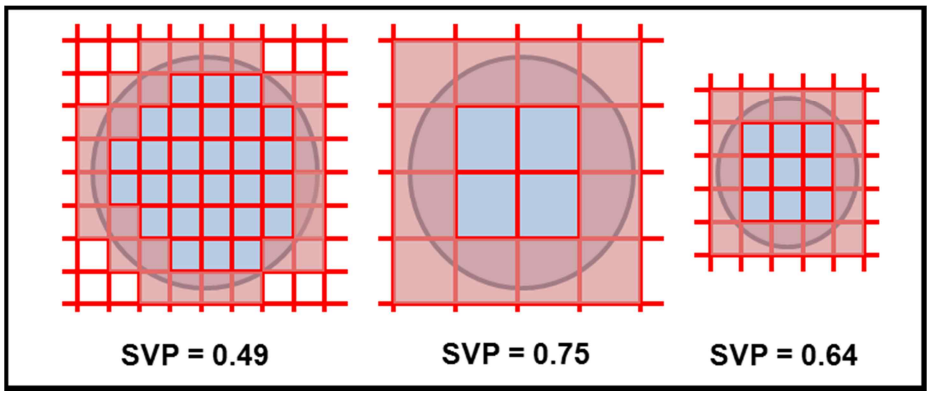

Figure 8. A diagrammatic example of changing *SVP* according to nodule volume and voxel size.

Increasing volume of nodule with same voxel size may cause decrease in *SVP*, while increasing size of voxel with same nodule volume may cause increase in *SVP*

REFERENCES

1. Crow J, Slavin G, Kreel L. Pulmonary metastasis: a pathologic and radiologic study. Cancer. 1981;47(11):2595-602.
2. Hasegawa M, Sone S, Takashima S, Li F, Yang ZG, Maruyama Y, et al. Growth rate of small lung cancers detected on mass CT screening. The British journal of radiology. 2000;73(876):1252-9.
3. Jaffe CC. Measures of response: RECIST, WHO, and new alternatives. Journal of clinical oncology : official journal of the American Society of Clinical Oncology. 2006;24(20):3245-51.
4. Oxnard GR, Zhao B, Sima CS, Ginsberg MS, James LP, Lefkowitz RA, et al. Variability of lung tumor measurements on repeat computed tomography scans taken within 15 minutes. Journal of clinical oncology : official journal of the American Society of Clinical Oncology. 2011;29(23):3114-9.
5. Revel MP, Lefort C, Bissery A, Bienvenu M, Aycard L, Chatellier G, et al. Pulmonary nodules: preliminary experience with three-dimensional evaluation. Radiology. 2004;231(2):459-66.
6. Therasse P, Arbuck SG, Eisenhauer EA, Wanders J, Kaplan RS, Rubinstein L, et al. New guidelines to evaluate the response to treatment in solid tumors. European Organization for Research and Treatment of Cancer, National Cancer Institute of the United States, National Cancer Institute of Canada. Journal of the National Cancer

Institute. 2000;92(3):205-16.

7. Buckler AJ, Schwartz LH, Petrick N, McNitt-Gray M, Zhao B, Fenimore C, et al. Data sets for the qualification of volumetric CT as a quantitative imaging biomarker in lung cancer. Optics express. 2010;18(14):15267-82.

8. Yankelevitz DF, Reeves AP, Kostis WJ, Zhao B, Henschke CI. Small pulmonary nodules: volumetrically determined growth rates based on CT evaluation. Radiology. 2000;217(1):251-6.

9. Zhao B, Schwartz LH, Moskowitz CS, Ginsberg MS, Rizvi NA, Kris MG. Lung cancer: computerized quantification of tumor response--initial results. Radiology. 2006;241(3):892-8.

10. Gietema HA, Schaefer-Prokop CM, Mali WP, Groenewegen G, Prokop M. Pulmonary nodules: Interscan variability of semiautomated volume measurements with multisection CT--influence of inspiration level, nodule size, and segmentation performance. Radiology. 2007;245(3):888-94.

11. Goodman LR, Gulsun M, Washington L, Nagy PG, Piacsek KL. Inherent variability of CT lung nodule measurements in vivo using semiautomated volumetric measurements. AJR American journal of roentgenology. 2006;186(4):989-94.

12. Wormanns D, Kohl G, Klotz E, Marheine A, Beyer F, Heindel W, et al. Volumetric measurements of pulmonary nodules at multi-row detector CT: in vivo reproducibility. European radiology. 2004;14(1):86-92.

13. Zhao B, James LP, Moskowitz CS, Guo P, Ginsberg MS, Lefkowitz RA, et al. Evaluating variability in tumor measurements from same-day repeat CT scans of patients with non-small cell lung cancer. Radiology. 2009;252(1):263-72.

14. Goo JM, Tongdee T, Tongdee R, Yeo K, Hildebolt CF, Bae KT. Volumetric measurement of synthetic lung nodules with multi-detector row CT: effect of various image reconstruction parameters and segmentation thresholds on measurement accuracy. Radiology. 2005;235(3):850-6.

15. Ko JP, Rusinek H, Jacobs EL, Babb JS, Betke M, McGuinness G, et al. Small pulmonary nodules: volume measurement at chest CT--phantom study. Radiology. 2003;228(3):864-70.

16. Marten K, Funke M, Engelke C. Flat panel detector-based volumetric CT: prototype evaluation with volumetry of small artificial nodules in a pulmonary phantom. Journal of thoracic imaging. 2004;19(3):156-63.

17. Petrou M, Quint LE, Nan B, Baker LH. Pulmonary nodule volumetric measurement variability as a function of CT slice thickness and nodule morphology. AJR American journal of roentgenology. 2007;188(2):306-12.

18. van Klaveren RJ, Oudkerk M, Prokop M, Scholten ET, Nackaerts K, Vernhout R, et al. Management of lung nodules detected by volume CT scanning. The New England journal of medicine. 2009;361(23):2221-9.

19. Goo JM. A computer-aided diagnosis for evaluating lung nodules on chest CT: the current status and perspective. Korean journal of radiology : official journal of the Korean Radiological Society. 2011;12(2):145-55.

20. Kostis WJ, Reeves AP, Yankelevitz DF, Henschke CI. Three-dimensional segmentation and growth-rate estimation of small pulmonary nodules in helical CT images. IEEE transactions on medical imaging. 2003;22(10):1259-74.

21. de Hoop B, Gietema H, van Ginneken B, Zanen P, Groenewegen G, Prokop M. A comparison of six software packages for evaluation of solid lung nodules using semi-automated volumetry: what is the minimum increase in size to detect growth in repeated CT examinations. European radiology. 2009;19(4):800-8.

22. Wadell H. Volume, shape, and roundness of quartz particles. J Geol. 1935;43(3):250-80.

23. Marrie RA, Dawson NV, Garland A. Quantile regression and restricted cubic splines are useful for exploring relationships between continuous variables. Journal of clinical epidemiology. 2009;62(5):511-7 e1.

24. Cade BS, Noon BR. A gentle introduction to quantile regression for ecologists. Front Ecol Environ. 2003;1(8):412-20.

25. Gavrielides MA, Kinnard LM, Myers KJ, Petrick N. Noncalcified lung nodules: volumetric assessment with thoracic CT. Radiology. 2009;251(1):26-37.

26. Reeves AP, Chan AB, Yankelevitz DF, Henschke CI, Kressler B, Kostis WJ. On measuring the change in size of pulmonary nodules. IEEE transactions on medical imaging. 2006;25(4):435-50.

27. Das M, Ley-Zaporozhan J, Gietema HA, Czech A, Muhlenbruch G, Mahnken AH, et al. Accuracy of automated volumetry of pulmonary nodules across different multislice CT scanners. European radiology. 2007;17(8):1979-84.

28. Kuhnigk JM, Dicken V, Zidowitz S, Bornemann L, Kuemmerlen B, Krass S, et al. Informatics in radiology (infoRAD): new tools for computer assistance in thoracic CT. Part 1. Functional analysis of lungs, lung lobes, and bronchopulmonary segments. Radiographics : a review publication of the Radiological Society of North America, Inc. 2005;25(2):525-36.

29. Kostis WJ, Yankelevitz DF, Reevez AP, Fluture SC, Henschke CI. Small pulmonary nodules: reproducibility of three-dimensional volumetric measurement and estimation of time to follow-up CT. Radiology. 2004;231(2):446-452.

30. Petkovska I, Brown MS, Goldin JG, Kim HJ, McNitt-Gray MF, Abtin FG, et al. The effect of lung volume on nodule size on CT. Academic radiology. 2007;14(4):476-85.

31. Weiss E, Wijesooriya K, Dill SV, Keall PJ. Tumor and normal tissue motion in the thorax during respiration: Analysis of volumetric and positional variations using 4D CT. International journal of radiation oncology, biology, physics. 2007;67(1):296-307.

32. Zwirewich CV, Vedal S, Miller RR, Muller NL. Solitary pulmonary nodule: high-resolution CT and radiologic-pathologic correlation. Radiology. 1991;179(2):469-76.

국문 초록

서론: 반자동 폐결절 용적측정은 폐결절 용적 변화를 조기에 발견함으로써 악성 결절의 진단 및 치료 반응 평가에 유용할 것으로 기대되고 있다. 그러나 폐결절 용적 측정의 측정 오차는 다양한 인자에 의해 영향을 받는 것으로 알려져 있다. 본 연구에서는 전이성 폐결절을 동반한 환자에서 반복 촬영 전산화 단층을 통하여 폐결절 용적 측정의 측정 변이 범위를 예측 및 모델링하고자 하였다.

방법: 2013 년 11 월부터 2014 년 4 월까지, 50 명의 전이성 폐결절을 갖는 환자를 전향적으로 모집하였다. 환자의 동의 하에, 같은 날, 10 분 이내의 간격으로 두 차례의 비조영 흉부 전산화 단층촬영 (Computed tomography, CT)을 반복 촬영하였다. 폐결절 직경 4 mm 에서 15 mm 사이의 결절을 대상으로 각 CT 를 대상으로 자체 용적 측정 소프트웨어를 이용하여 폐결절 분할을 시행하였고, 분할된 폐결절의 평균 용적 (mean nodule volume, V_m)을 얻었다. 표면 화적소 분율 (Surface voxel proportion, *SVP*)를 분할된 전체 화적소 수 중 결절 표면에 위치한 화적소 수의 분율로, 접합 분율 $_N$ (Attachment proportion, AP_N)을 결절 표면 바로 바깥쪽에 위치한 화적소 중 감쇄값 N 이상의 값을 갖는 화적소의 분율로 정의하였다. 이후 측정된 결절 용적을 절대 백분위 오차 (Absolute percentage error, *APE*) 및 상대 백분위 오차 (Relative percentage error,

RPE)를 계산하였다. 측정오차의 상위 95% 한계를 예측하기 위하여 Quantile 회귀 분석을 시행하였다.

결과: 상대 백분위 오차의 95% 변이 범위는 −20.81%부터 20.62%까지였다. 단변수 Quantile 회귀분석 상에서 평균 결절 용적, Sphericity, 표면 화적소 분율 및 접합 분율$_{-700}$, 접합 분율$_{-600}$ 이 유의한 예측 인자로 나타났다. 다변수 분석 상에서는 표면 화적소 분율과 접합 분율$_{-700}$ 이 모델의 유의한 변수로 채택되었으며 절대 백분위 오차의 95% 상한치는 다음의 식으로 예측할 수 있다. $APE = 46.01 \cdot SVP + 36.32 \cdot AP_{-700} - 12.94$.

결론: 표면 화적소 분율과 접합 분율은 폐결절 용적 측정의 변이 범위 예측의 유의한 독립적 인자였으며 이 두 변수를 이용한 모델을 통하여 폐결절 용적 측정 오차의 95% 상한을 예측할 수 있었다.

주요어 : 전산화 단층 촬영, 폐결절, 측정 오차, 용적 측정, 모델링
학 번 : 2012-23629